UCLA
UCLA Previously Published Works

Title
Why Boron Nitride is such a Selective Catalyst for the Oxidative Dehydrogenation of Propane

Permalink
https://escholarship.org/uc/item/4n99b982

Journal
Angewandte Chemie International Edition, 59(38)

ISSN
1433-7851

Authors
Venegas, Juan M
Zhang, Zisheng
Agbi, Theodore O
et al.

Publication Date
2020-09-14

DOI
10.1002/anie.202003695

Peer reviewed

Why Boron Nitride is such a Selective Catalyst for the Oxidative Dehydrogenation of Propane

Juan M. Venegas[a]†‡, Zisheng Zhang[b]‡, Theodore O. Agbi[a], William P. McDermott[c], Anastassia Alexandrova[b]*, Ive Hermans[a,c]*

[a] Dr. J.M. Venegas, T. O. Agbi, Prof. Dr. I. Hermans
     Department of Chemical and Biological Engineering,
     University of Wisconsin – Madison,
     1415 Engineering Drive, Madison, Wisconsin 53706, United States
     E-mail: hermans@chem.wisc.edu
[b] Z. Zisheng, Prof. Dr. A. Alexandrova
     Department of Chemistry and Biochemistry,
     University of California, Los Angeles,
     607 Charles E. Young Drive, Los Angeles, California 90095, United States
     Email: ana@chem.ucla.edu
[c] W. P. McDermott, Prof. Dr. I. Hermans
     Department of Chemistry,
     University of Wisconsin – Madison
     1101 University Avenue, Madison, Wisconsin 53706, United States

     † Present address: Performance Silicones Process R&D
     The Dow Chemical Company
     2651 W. Salzburg Road, Midland, Michigan 48640, United States

     ‡authors contributed equally

     Supporting information for this article is given via a link at the end of the document.

Abstract: In recent years, boron-containing materials and in particular boron nitride, have been identified as highly selective catalysts for the oxidative dehydrogenation of alkanes such as propane. Until now, no mechanism exists that can explain both the unprecedented selectivity, the observed surface oxyfunctionalization, as well as the peculiar kinetic features of the reaction. In this contribution we combine catalytic activity measurements with quantum chemical calculations to put forward a bold new hypothesis. Based on our results, we argue that the remarkable product distribution can be rationalized by a combination of surface-mediated formation of radicals over metastable sites, and their sequential propagation in the gas phase. Based on known radical propagation steps, we quantitatively describe the oxygen pressure-dependent relative formation of the main product propylene and by-product ethylene. The free radical intermediates are most likely what differentiates this catalytic system from less selective vanadium-based catalysts. Indeed, although the mechanism of this benchmark catalyst is also not yet unambiguously established, it is generally assumed that radical intermediates are rapidly converted to stable molecular products on the catalyst surface before they can desorb. The new insights obtained in this work highlight the importance of the mechanistic differences between these two catalyst families, which could lead to better design principles and improved catalytic systems.

Introduction

Hexagonal boron nitride (hBN) and other boron-containing materials recently emerged as promising catalysts for the oxidative dehydrogenation (ODH) of small alkanes, due to their unprecedented high olefin selectivity.[1] Breakthroughs in ODH research could drastically reduce the energy that is required in the synthesis of building block olefins. It has been shown that the oxidation of the catalyst surface to an amorphous boron hydroxy oxide layer is not only crucial for ODH activity, the surface composition of these boron-based materials is highly dynamic and sensitive to the reaction conditions.[7–9] Kinetic studies have shown that the predominance of dehydrogenation versus C-C bond cleavage – the most important side-reaction – is controlled by the oxygen concentration.[10,11] To rationalize many of these observations, we explored the possible role of gas phase chemistry and found strong experimental indications of surface-initiated gas-phase radical reactions. It is for instance observed that the ODH reactivity scales with total packed bed volume rather than the hBN mass only, and that for a give bed volume the reaction rate features a maximum as a function of the hBN loading.[12] These observations are at odds with a pure surface-catalyzed reaction but rather suggest a free-radical mediated mechanism that can be both initiated and quenched by catalytic species.[13] Very recently, Zhang, *et al.* successfully detected radicals during the ODH of propane using hBN catalysts *via* synchrotron vacuum ultraviolet photoionization mass spec- troscopy (SVUV-PIMS), in support of this hypothesis.[14]

Considering the possible radical pathways involved in hBN-catalyzed ODH, we aim to gain insight into the reactions that could take place both at the surface and in the gas phase. Additionally, the role of H_2O has not been extensively explored to date, despite it being a significant reaction product and literature precedent

suggesting its possible synergistic role in improving oxidation performance.[15,16] Gas phase alkane oxidation chemistry features complex radical-based reaction networks, and this contribution extracts the key features of these reaction mechanisms that can explain the unique performance of boron-based ODH catalysts.

Results and Discussion

Steam enhances the ODH activity for boron nitride
We start by investigating the difference in reactivity of hBN under standard conditions ('dry'; without water added to the reaction feed) and 'wet' conditions where 10% water vapor was cofed. All experimental details can be found in the Supporting Information. Figure 1 shows the rate dependence on C_3H_8 during ODH under dry and wet conditions at a constant total flow of 50 mL_{STP} min^{-1} and differential propane conversions ($X < 10\%$). Under both feed conditions we observe an apparent order 2.1±0.1 in propane, with the wet stream leading to higher reaction rates at all C_3H_8 concentrations. This observed rate-enhancement stands in strong contrast to the inhibiting effect of water that has been reported for supported vanadium ODH catalysts.[17,18]

If the observed increase in reactivity upon the addition of steam were due to alkane conversion by new reaction pathways, we would expect differences in conversion-selectivity trends between dry and wet conditions. Instead, Figure 2 shows that the selectivity towards C_3H_6 – at a given conversion – is independent of the addition of steam. It appears then, that the addition of water enhances the rates of pathways already present under standard conditions. To complement these observed activity improvements with wet ODH feeds, we varied water concentrations between 1-20 mol% under two propane concentrations (15 and 25 mol%, Figure S1). These experiments show a linear increase in propane consumption rates with water content, suggesting water is indeed involved in the formation of reactive species during ODH.
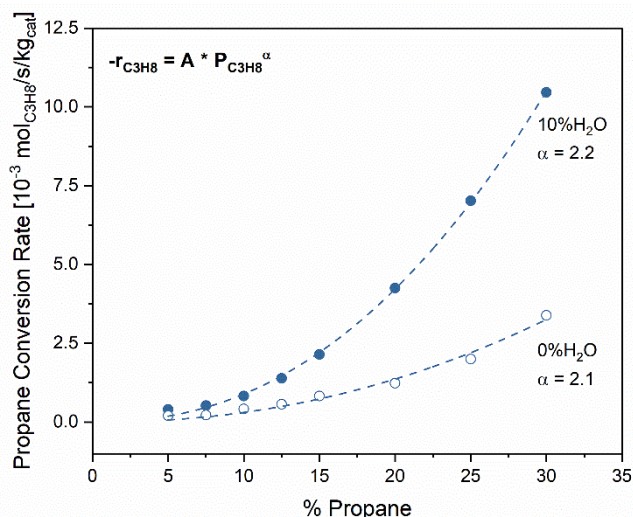
Figure 1. Propane conversion rate as a function of propane concentration with water cofeed (solid symbols) and under standard feed conditions (open symbols). Reaction conditions: T = 525 °C, Total flow = 50 mL_{STP} min^{-1}, Feed composition: 15% O_2, 5-30% C_3H_8, balance N_2. During water cofeed, N_2 flow rates were adjusted to obtain 10% H_2O concentration. α denotes the exponent used to obtain the fitted curve from the power law equation $-r_{C3H8} = A * P_{O2}^{\alpha}$.

The second-order rate-dependence on C_3H_8 has been a characteristic feature of B-catalyzed ODH.[1,3] This nonlinear dependence can be explained within the context of a mixed surface-gas phase mechanism. When using MgO-based catalysts, Leveles et al. hypothesized that at low alkane concentrations, the gas-phase contribution to propane conversion can be neglected, relative to surface reactions.[19] Under alkane-rich feeds, however, gas phase radical chemistry leading to propane H-abstraction becomes comparable to surface-mediated propane activation in its contribution to the overall ODH activity. In the present work, the rate enhancement observed upon the co-feed of steam indicates that water may be involved in formation of intermediates that react in the gas-phase.
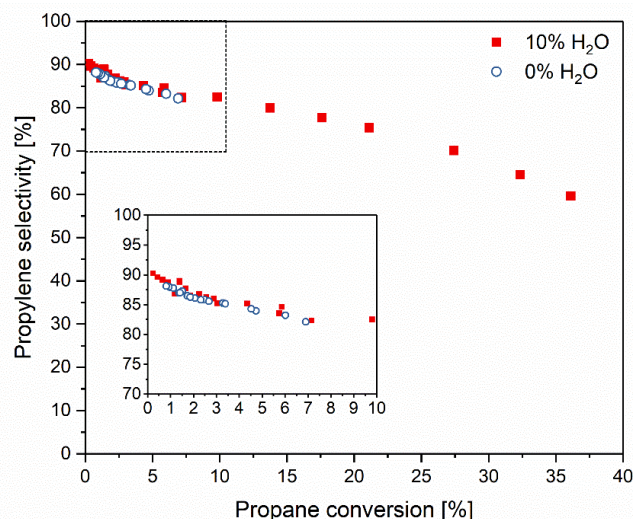

Figure 2. Propylene selectivity as a function of propane conversion during water cofeeding (red symbols) and under standard feed conditions (open blue symbols). Inset details conversions below 10%. Reaction conditions: T = 525 °C, Total flow = 20-80 mL_{STP} min^{-1}, Feed composition = 15% O_2, 5-30% C_3H_8, balance N_2. During water cofeed, N_2 flow rates were adjusted to obtain 10% H_2O concentration.

After establishing the synergistic role of water in ODH, we studied the reversibility of its rate-enhancement by cycling 'dry' and 'wet' conditions over a period of ~4 days. During a cycle, the catalyst was exposed to either wet or dry streams (using a 6-way valve to switch streams with minimal flow disturbance) for 12 hours. If irreversible structural changes would occur due to the presence of added steam, we hypothesize that the steady-state reactivity of the catalyst would evolve with time. For example, if water-induced surface

modifications would irreversibly lead to more active sites, we would expect steady-state reactivity under dry conditions to increase at a given flow condition. *Vice versa*, the inhibition of surface species would decrease reactivity as previously observed for supported vanadium catalysts.[17,18] If the effect of H_2O was only to alter the gas phase radical concentration, or if surface changes are reversible, the reactivity at each cycle would remain constant during the experiment. Figure 3 shows that during the 12-hour cycling periods, the propane conversion steadily increases (during a wet cycle) or decreases (during a dry cycle). However, the asymptotic conversion reached during all cycles remains constant at ~2-3% under dry conditions, and ~9-10% during wet feed cycles. Additionally, the observed propylene selectivity during each cycle also remains constant at 85% and 80% during dry and wet cycles, respectively, consistent with the difference in conversion (full product distribution under each condition is provided in Figure S2).
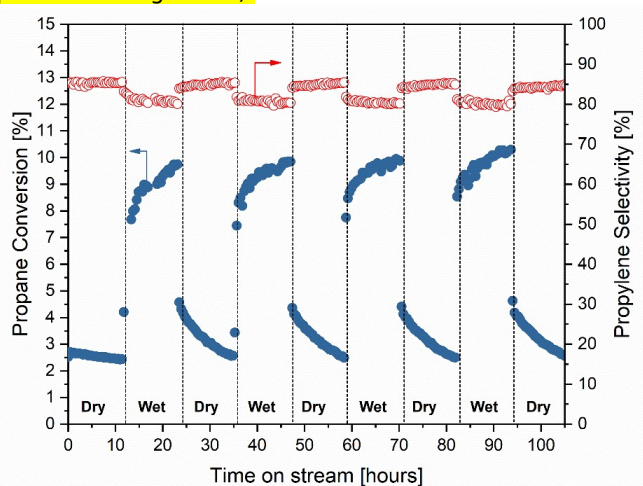

Figure 3. Propane conversion (blue symbols, left axis) and propylene selectivity (red symbols, right axis) as a function of time on-stream during 12-hour cycles of 'wet' or 'dry' ODH feed. Prior to cycling, the catalyst had undergone ODH under wet conditions for 24 hours, and subsequently ODH under dry conditions for 24 hours. $T = 525$ °C, $F_{total} = 40$ mL$_{STP}$ min^{-1}. Dry feed = 30% C_3H_8, 15% O_2, 55% N_2. Wet feed = 30% C_3H_8, 15% O_2, 45% N_2, 10% H_2O.

The cycling experiment may provide insights into various effects water has on the observed reactivity. ~70% of the total conversion change happens within the first hour of a cycle. The remaining conversion change occurs throughout the remaining time of the cycle, *circa* 11 hours. These different time scales suggest that water influences the observed reactivity by multiple routes. The high reactivity of radicals suggests that the rapid conversion change may be due to the formation or disappearance of a radical source. As the only difference between cycles is the addition of water, we hypothesize that these radicals stem from the activation of H_2O. The second role of water, which leads to the slower change in propane conversion, is unlikely to involve radicals. This longer time scale effect may involve changes in the concentration of active surface species. This role is supported by the constant conversion-selectivity trends in Figure 2, indicating that no new reaction pathways

are enabled. As such, a remaining possibility lies in changes in the concentration of active surface species.

After establishing the reversible nature of water's effect on ODH activity, we assessed whether water may be directly involved in C_3H_8 conversion *via* an oxygen cutoff experiment (Figure 4). In this test, we performed ODH under wet conditions until stable propane conversion was observed, and oxygen was subsequently removed from the reaction feed. Within the timescale of our GC analysis (*i.e.* ~25 minutes), we see a complete loss of catalytic activity under anaerobic conditions. This experiment indicates that oxygen-derived intermediates are necessary to form reactive species from H_2O. These observations remind us of the work by Takanabe and Iglesia that suggest that chemisorption and activation of O_2 is necessary for the subsequent activation of CH_4 and H_2O under wet oxidative coupling of methane (OCM) over a Mn/Na$_2$WO$_4$/SiO$_2$ catalyst.[15]
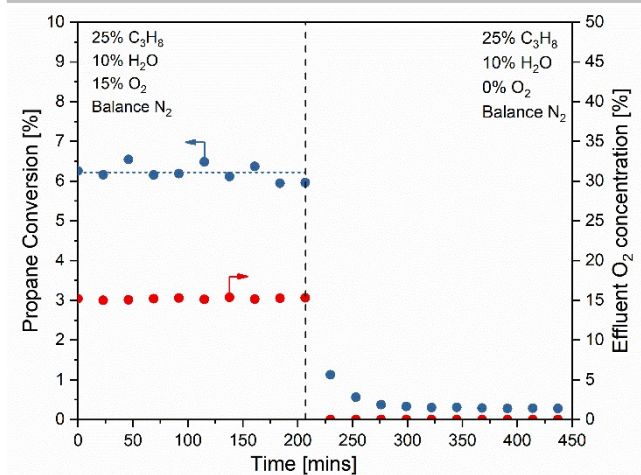
Figure 4. Oxygen cut-off experiment. ODH under a wet reaction feed was run for ~200 minutes, after which O_2 was removed from the reactor feed and the resulting catalytic activity was monitored. Blue symbols represent observed propane conversion (left axis) and red symbols represent oxygen concentration as determined by GC (right axis).

Oxygen is not only required to observe activity, but its concentration also determines the selectivity during ODH. Figure S3 shows changes in product distribution at varying oxygen feed concentrations. In line with previous reports,[5,10] under oxygen lean conditions, C-C cracking pathways to produce C_2H_4 become increasingly important. These trends hold using both dry and wet ODH feeds, highlighting once again the possible role of water in enhancing reaction rates already present rather than enabling new reaction pathways. In the context of a surface-mediated gas phase reaction network, the types of radicals formed may provide rationale behind these observed selectivity trends as discussed below.
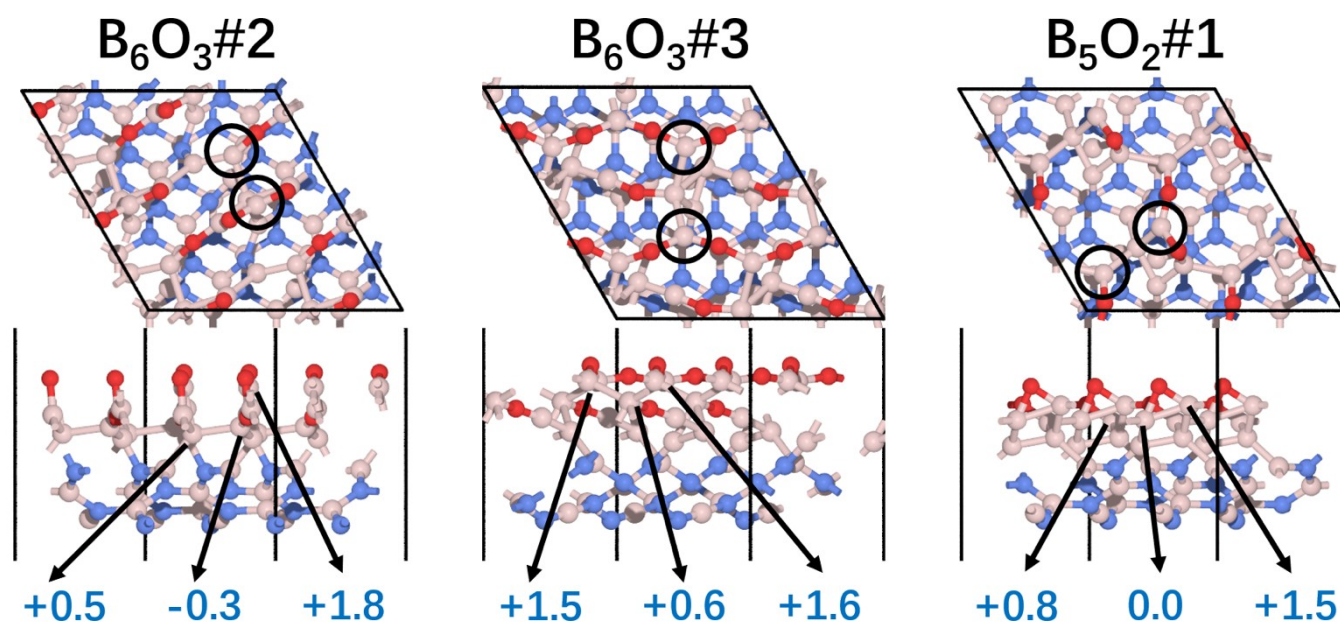
B$_6$O$_3$#2   B$_6$O$_3$#3   B$_5$O$_2$#1

+0.5   -0.3   +1.8   +1.5   +0.6   +1.6   +0.8   0.0   +1.5

Figure 5. Top and side view of the three surface states studied in this work: B$_6$O$_3$#2, B$_6$O$_3$#3, and B$_5$O$_2$#1. Bader charge of key atoms in the {BB} motif is labeled under side view of each surface state in blue text. Color code: Pink = boron, blue = nitrogen, red = oxygen.

Computational insights

Our previous experimental studies show that the surface of boron-based catalysts oxyfunctionalizes during ODH chemistry, but it remained unclear which species in the amorphous hydroxy oxide layer could be responsible for the observed activity.[7,8] The fact that site-isolated BO$_3$-species with saturated and fully oxidized local environments as created in a zeolite matrix (*viz.* B-MWW) are inactive for ODH suggest that the amorphous hydroxy oxide network is actually key.[20] This hypothesis is further supported by the fact that impregnation of boron onto the inactive B-MWW resulted in an active catalyst (B/B-MWW) featuring B-O-B connectivity.[20] We emphasize that this amorphous interface is highly dynamic, and as such it is a suspect for presenting metastable active sites. Metastable species may remain a minority, and thus poorly detectable even by *operando* characterization.[21,22] Such active sites may be studied by leveraging computational tools. Previous theoretical work reveals a dynamic BO$_x$ surface which indeed contains metastable surface states with distinct geometries, stoichiometries, and chemistries, which can form on a timescale of picoseconds, and become only significantly populated as the temperature is increased from 298 K to 763 K, based on grand canonical simulations.[9] After ruling out the BO$_3$-type surface units, we obtained three other types of sites that have >5% population at the reaction temperature; all of them contain unsaturated B-B-B units in which the middle B is buried in the sublayer while two ends are exposed (denoted as {BB}). These sites (shown in Figure 5) can be found in the global minimum of the B$_5$O$_2$ phase (B$_5$O$_2$#1), and the second and third local minimum of the B$_6$O$_3$ phase (B$_6$O$_3$#2, B$_6$O$_3$#3). The calculated Bader charges of these species (Figure 5) show distinct electronic environments compared to BN$_3$

or BO$_3$ (Bader charge: +2.2), which suggest unusual chemical reactivities.

As oxygen is critical to ODH, we first explored a possible route to O$_2$ activation on {BB} surface species. O$_2$ chemisorption on {BB} is thermodynamically favorable for all three surface states, and forms barrierless peroxo-like >BO-OB< species. The >BO-OB< cleavage is then explored in B$_6$O$_3$#2, B$_6$O$_3$#3, and B$_5$O$_2$#1. Figure 6 shows the facile O-O bond cleavage (energy barrier of only 49 kJ/mol) to form >B-O• surface species in B$_6$O$_3$#2. This reaction path is similar to those proposed by Aparicio *et al.* during OCM with Li-doped MgO catalysts, with the formed MO• abstracting H-atoms from methane.[23] As expected, the formed BO• species depicted in Figure 6 are highly reactive, readily forming both *i*-propyl (barrierless) and *n*-propyl (5.3 kJ/mol barrier) radicals from propane plus BOH surface groups (Figure S4). However, the B$_6$O$_3$#3 and B$_5$O$_2$#1 get further oxidized upon cleavage of >BO-OB< by rapidly interacting with proximate B atoms, and therefore not producing stable BO• sites.

In parallel to the formation of propyl radicals *via* the activation of O$_2$ as detailed in Figure S4, we also set out to understand the effect of water. We first investigated how water may interact with the catalyst surface (Figure S5), and the three surface states show very similar behaviors. Upon interaction of water with a {BB} site, the O-H bond in water is lengthened by interactions with a proximate B-atom. The calculated transition state related to O-H bond breaking has a barrier of 57 kJ/mol, 66 kJ/mol, and 89 kJ/mol, for B$_6$O$_3$#2, B$_6$O$_3$#3, and B$_5$O$_2$#1, respectively. At this point, the B where water adsorption took place adopts the BO$_3$ geometry and is repelled away from the newly formed BH species, with an overall ΔG of -251 kJ/mol, -199 kJ/mol, and -123 kJ/mol for B$_6$O$_3$#2, B$_6$O$_3$#3, and B$_5$O$_2$#1, respectively.

5

While valuable to assess the role of water under ODH conditions, the predicted pathways do not lead to BO_x species. >BH does not appear to be reactive for H-abstraction, and our oxygen cutoff experiment (Figure 4) suggests that, under wet conditions, propane conversion still requires the presence of oxygen. The likely fate of the formed B-H species is therefore the reaction with O_2 to form HOO• radicals (reaction 1). These HOO• radicals subsequently abstract H-atoms from the propane substrate leading to more propyl radicals.

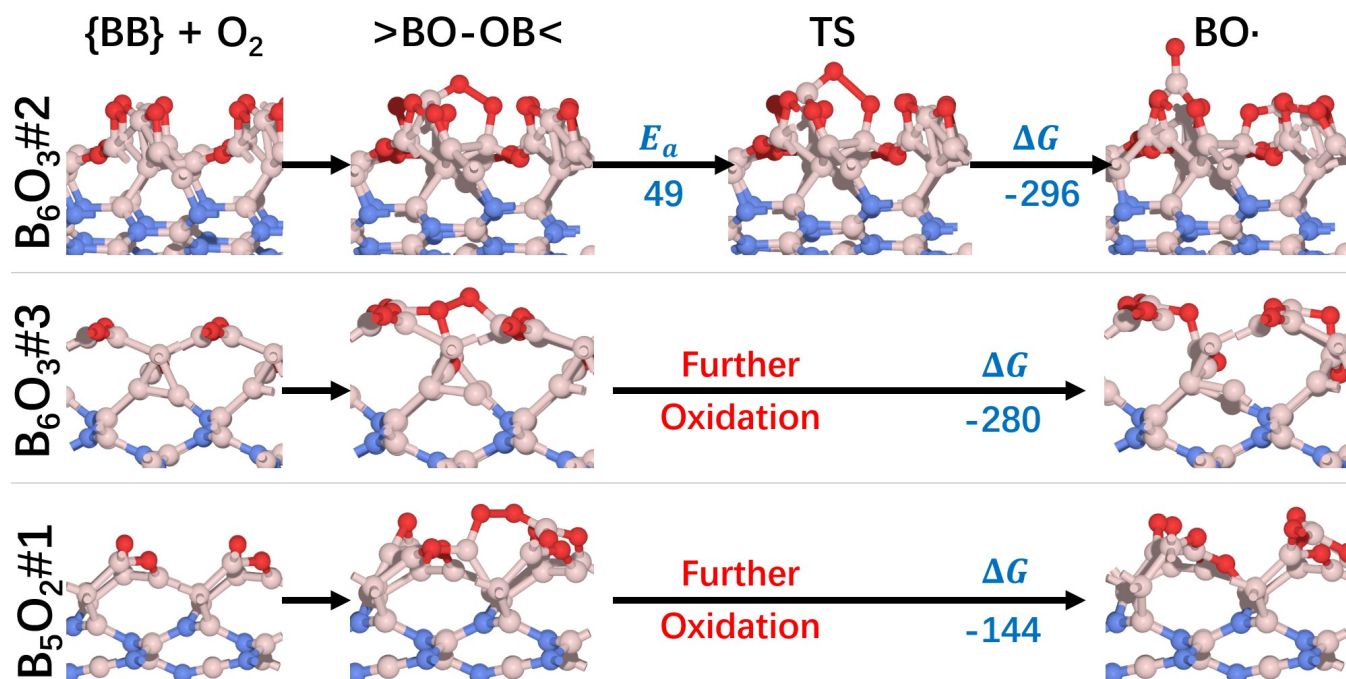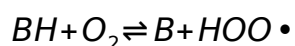$$BH + O_2 \rightleftharpoons B + HOO\bullet \qquad\qquad (1)$$

Figure 6. Structural models showing O_2 chemisorption and activation on B_6O_3#2, B_6O_3#3, and B_5O_2#1. The chemisorption steps are all barrierless. The activation energy and overall ΔG values (in kJ/mol) are labeled on connecting arrows. Color code: Pink = boron, blue = nitrogen, red = oxygen, white = hydrogen.
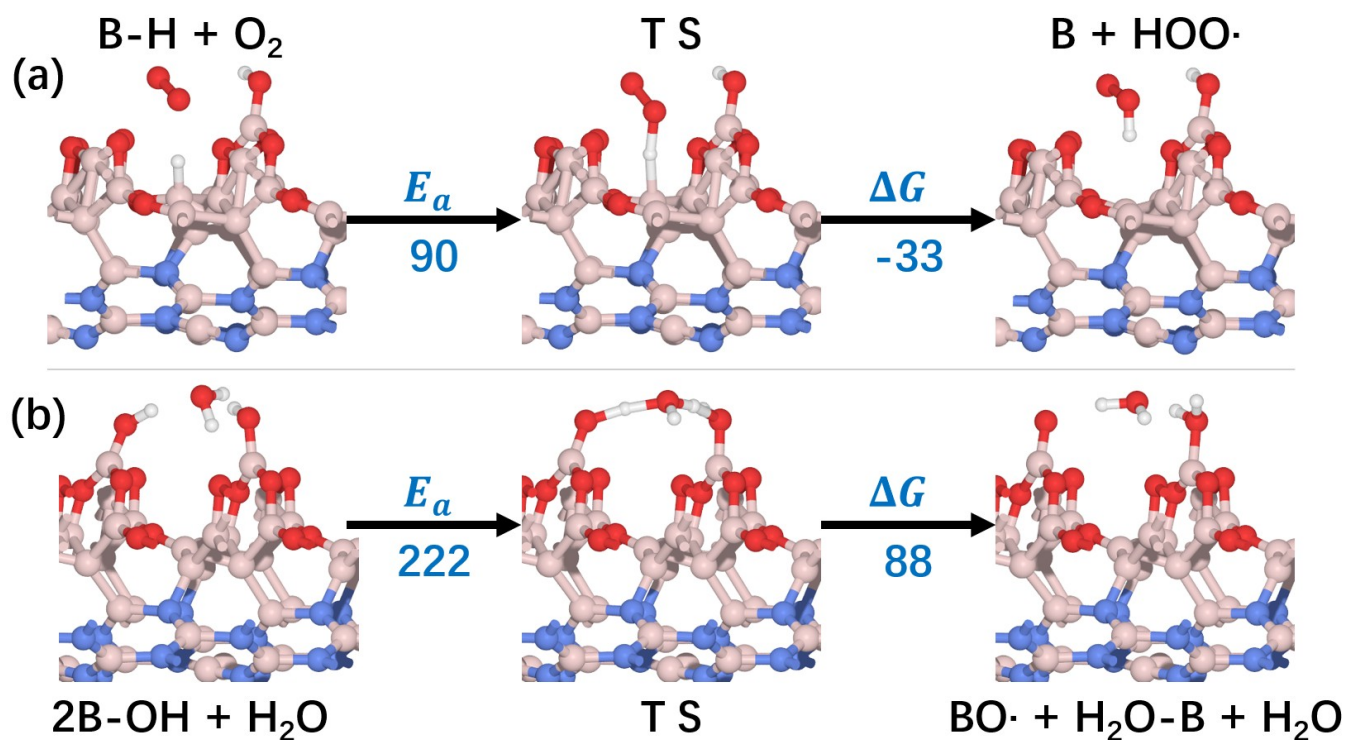

Figure 7. Structural models showing (a) initiation of HOO• radical from surface BH and gas phase O_2 and (b) regeneration of surface BO• sites from BOH species mediated by a bridging water molecule in B_6O_3#2. The activation energy and overall ΔG values (in kJ/mol) are labeled on connecting arrows. Color code: Pink = boron, blue = nitrogen, red = oxygen, white = hydrogen.

7

Our calculation shows that only B_6O_3#2 can achieve such a reaction, and the predicted pathway for O_2 interaction with >BH in B_6O_3#2 is shown in Figure 7a. This reaction has a computed barrier of 90 kJ/mol and an overall ΔG = -33 kJ/mol. As such, surface sites derived from water activation still require O_2 to form the species capable of H-abstraction from propane in the gas-phase. This readily explains why the catalyst shows no dehydrogenation activity and is only active for ODH.

From above explorations of the elemental steps on three potential "hot" active sites, we find that all of them can contribute to the whole map of catalysis to some extent. B_6O_3#2 stands out as the candidate that can chemisorb and activate O_2 into stable BO• to abstract an H-atom from propane as well as activate water into B-H that can react with O_2 to form a free HOO• radical. The barrier for water dissociation in B_6O_3#2 is also lower than those in B_6O_3#3 and B_5O_2#1, suggesting B_6O_3#2 may be the main contributor to water activation.
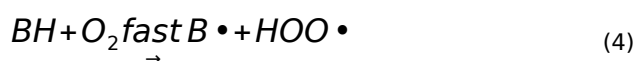
The property of B_6O_3#2 can be attributed to the electronic structure of the B in {BB} motif, and its unique geometry, as is shown in Figure 5. The middle B atom in the {BB} of B_6O_3#2 features an unusual Bader charge of -0.3, suggesting a higher electron density than those in B_6O_3#3 (Bader charge: +0.6) and B_5O_2#1 (Bader charge: 0.0). Moreover, in B_6O_3#2, the top-layer B and O atoms are arranged into chains of B_4O_2 units while the sub-layer are relatively rigid, unlike the sublayer of B_6O_3#3 and B_5O_2#1 which contain messy unidirectional B-B motifs that leave the surface prone to structural deformation and further oxidation.

After determining the major active surface species and possible routes for the generation of free radicals *via* surface reactions, we investigated the role surface species may have in radical quenching. We previously reported on the effect of varying catalyst mass within a given packed bed volume.[12] For a given set of reaction conditions, there is a volcano-type dependence of the reaction rate on catalyst mass, suggesting a balance between surface-derived radical-generation and -termination events. To test this hypothesis, we investigated interactions between the >BO• species formed upon O_2 dissociative adsorption and gas phase radical species. As O_2 in the gas phase is likely to interact with propyl species formed after propane activation, forming HOO• radicals (*vide infra*), we assessed their possible quenching reaction on the catalyst surface. Figure S6 describes the reaction of gas phase HOO• with a surface >BO• species to form BOH and an O_2 molecule. This reaction is barrierless, with an overall ΔG = -94 kJ/mol. As such, surface quenching of radicals likely modulates the overall concentration of radicals available for gas phase chemistry, as well as the concentration of reactive >BO• species on the surface.

H-abstraction from propane by >BO• leads to the formation of BOH surface species which have been verified experimentally in previous investigations.[1,8,24] These sites, however, are expected to be fairly unreactive, and as such we investigated active site regeneration. Starting from the experimental

observation that water enhances the observed reaction rate at all studied reaction conditions, we assessed the possibility of water enabling active site regeneration. More specifically we envisioned the dehydration of two >BOH sites, mediated by water. In this scenario, a water molecule bridges between two BOH groups that are ~5 Å apart *via* hydrogen bonding, enabling proton transfer and subsequent surface dehydration (Figure 7b). This reaction leads to the formation of a >BO•, and an adsorbed H_2O-B with an E_a = 220 kJ/mol and an overall ΔG = 88 kJ/mol. The newly formed water desorbs from the surface in a consecutive step with ΔG of 61 kJ/mol, and the initial {BB} site is recovered to close the loop (Figure S8). The activation energy of this water-mediated surface regeneration process is compatible with experimentally reported apparent activation energies for hBN-catalyzed ODH in the 200-250 kJ/mol range.[6,25,26] We therefore hypothesize that this water-mediated site regeneration is the rate-limiting reaction in the overall ODH reaction, and not the H-abstraction from the alkane substrate as hypothesized for vanadium.[17,27]

Summarizing the findings from our computational studies, we identified two radical initiation mechanisms (2) and (3-4):

$$\{BB\} + O_2 \xrightarrow{k_{init,O2}} BOOB \xrightarrow{fast} 2\,BO\bullet \tag{2}$$

$$\{BB\} + H_2O \xrightarrow{k_{init,H2O}} BOH + BH \tag{3}$$

$$BH + O_2 \xrightarrow{fast} B\bullet + HOO\bullet \tag{4}$$

In addition, the high activation barrier for the water-assisted surface regeneration reaction 5 described in Figure 7b, suggests that regeneration of reactive BO• and B• species is rate controlling. This hypothesis is in line with the observed first-order rate-dependence in water (Fig. S1).

$$BOH + BOH \xrightarrow{H_2O} BO\bullet + B\bullet + H_2O \tag{5}$$
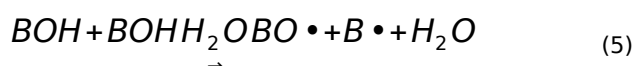
The radicals generated during the ODH reaction can terminate according to two pathways. First, in a radical-radical recombination reaction:
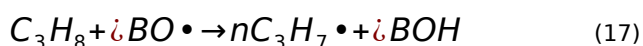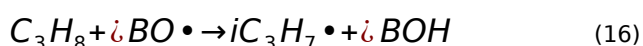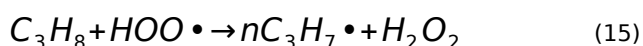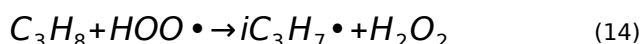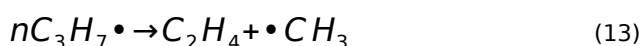
$$radical + radical \rightarrow non-radical\ product \tag{6}$$

Or in a surface termination reaction, with Figure S5 describing one predicted route:

$$¿BO\bullet + HOO\bullet \rightarrow >BOH + O_2 \tag{7}$$

We also note that, although only one of the candidate surface sites appears to possess the desired reactivity characteristics, there are likely more of them, because our exploration of the surface reconstruction under reaction conditions is limited by the size of the model and computational expense.

The role of gas phase chemistry on ODH performance

Building on the chemistry predicted to occur on the catalyst surface, we now investigate the possible gas-phase reaction network. <mark>Our aim for this model was to capture the key features of boron-catalyzed ODH (*i.e.* dehydrogenation versus cracking chemistry) with only the essential reaction network needed. As such, we focused on the first radicals formed from surface activation of propane and oxygen, which are likely critical in defining the selectivity of the ODH process.</mark> After surface activation of propane, both primary and secondary propyl radicals will react with molecular oxygen to form HOO• through a second H-abstraction step (reactions 8 and 9). This pathway is well-described in the combustion literature and stands in kinetic competition with another established reaction, namely unimolecular C-C bond cleavage (reactions 10-13). We can construct a simplified set of elementary steps to describe the primary formation of propylene from *n/i*-propyl radicals, the activation of propane in the gas phase *via* generated HOO•, as well as the main ODH side product, C_2H_4 under our reaction conditions:

$$O_2 + iC_3H_7• \rightarrow C_3H_6 + HOO• \tag{8}$$

$$O_2 + nC_3H_7• \rightarrow C_3H_6 + HOO• \tag{9}$$

$$iC_3H_7• \rightarrow C_3H_6 + •H \tag{10}$$

$$nC_3H_7• \rightarrow C_3H_6 + •H \tag{11}$$

$$iC_3H_7• \rightarrow C_2H_4 + •CH_3 \tag{12}$$

$$nC_3H_7• \rightarrow C_2H_4 + •CH_3 \tag{13}$$

$$C_3H_8 + HOO• \rightarrow iC_3H_7• + H_2O_2 \tag{14}$$

$$C_3H_8 + HOO• \rightarrow nC_3H_7• + H_2O_2 \tag{15}$$

$$C_3H_8 + iBO• \rightarrow iC_3H_7• + iBOH \tag{16}$$

$$C_3H_8 + iBO• \rightarrow nC_3H_7• + iBOH \tag{17}$$
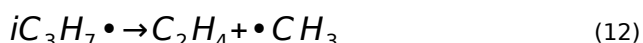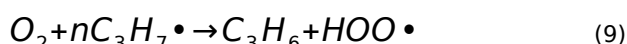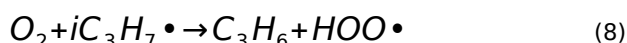
This well-established chemistry identifies HOO• as the predominant H-abstraction agent. We used rate coefficients compiled in the NIST Chemical Kinetics Database from various sources.[28-31] One can gauge the relative rate of C-H abstraction (leading to propylene) to C-C cracking (leading to ethylene) as a function of the oxygen partial pressure by equation 1 (derivation and rate constants in supporting information):

$$\frac{R_{C_3H_6}}{R_{C_2H_4}} = \frac{\left([O_2]\left(k_9 + \frac{k_8[iC_3H_7•]}{[nC_3H_7•]}\right) + k_{11} + \frac{k_{10}[i}{[nC}\right)}{\left(k_{13} + \frac{k_{12}[iC_3H_7•]}{[nC_3H_7•]}\right)} \tag{Eq. 1}$$

While the iC_3H_7/nC_3H_7 ratio is not directly experimentally accessible, we can evaluate equation 1 in two limiting scenarios: (1) Gas-phase activation of C_3H_8 *via* reactions 14 and 15, and (2) Surface activation of C_3H_8 *via* >BO• species formed from site B_6O_3#2 as described in Figure S4 (reactions 16 and 17). The rate coefficient ratio of reactions 14 and 15 leads to $iC_3H_7/nC_3H_7 = 1.5$, reflecting the slightly higher activation barriers reported for the abstraction of primary H-atoms by HOO• and the number of primary *vs* secondary H-atoms in propane. Similarly, we used the computed barriers for the surface H-abstraction by BO• to predict a $iC_3H_7/nC_3H_7 = 0.74$ under scenario 2, favoring the formation of *n*-propyl radicals. This result reflects the higher reactivity of BO• species relative to HOO• radicals, which makes the surface sites less selective for secondary C-H bonds in propane.

With equation 1, we compared the estimated R_{C3H6}/R_{C2H4} with the experimental ratio of C_3H_6 and C_2H_4 production rates while varying the O_2 partial pressure under different reaction conditions (Figure 8). We find that our experimental response up to 15% O_2 concentration lies between the limiting scenarios, with gas-phase propane activation (red line in Fig. 8) overestimating and surface activation (blue line in Fig. 8) underestimating the experimental ratios. When we vary the relative contributions of the surface and gas-phase propane H-abstraction to 42% and 58% respectively, we obtain good agreement between our model-predicted R_{C3H6}/R_{C2H4} ratio and the experimental observations within a broad O_2 concentration range (black line in Fig. 8). This model suggests that under ODH conditions, there may be a mix of surface and gas-phase propane H-abstraction, leading to an approximately equimolar amount of *i*-propyl and *n*-propyl radicals being formed. <mark>The H_2O_2 formed in reactions (14) and (15) is decomposed into water and oxygen,[14] or it can react barrierless with surface >BO• species to form additional HOO• radicals (see Fig. S7).</mark> Our proposed reaction mechanism <mark>(simplified schematic depicted in Figure 9)</mark> clearly highlights the importance of free radical gas-phase chemistry as well as surface-mediated reactions in explaining catalyst performance. This simple model is, to our knowledge, the first mechanistic hypothesis that can predict the experimentally observed product distribution of BO_x-catalyzed ODH over a range of oxygen partial pressures.
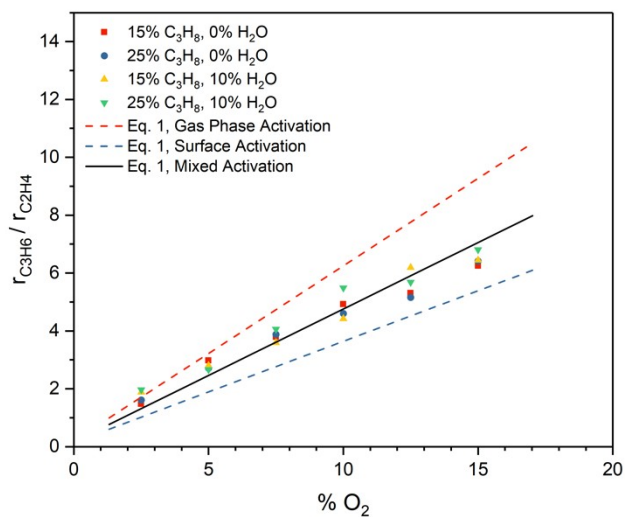
9

Figure 8. Comparison of experimental rates of propylene and ethylene formation as a function of O_2 concentration at T = 525°C. Lines are the calculated ratio between C_3H_6 and C_2H_4 production rates derived from equation 1 using three separate cases. Case 1 (red line): Propane activation by free HOO• radicals in gas-phase, leading to a iC_3H_7/nC_3H_7 = 1.5. Case 2 (blue line): Propane activation by surface BO• species, leading to a iC_3H_7/nC_3H_7 = 0.74. Case 3 (black line): Mixed activation by surface species (42%) and free HOO• radicals (58%), leading to a iC_3H_7/nC_3H_7 = 1.06. Ratio of overall r_{C3H6}/r_{C2H4} based on experimental rates of formation of propylene and ethylene. Propane conversions were kept below 5% under all conditions to approximate differential conditions.

According to this simple model, propane is consumed in reactions (14)-(17), leading to the following expression for the propane consumption:

10
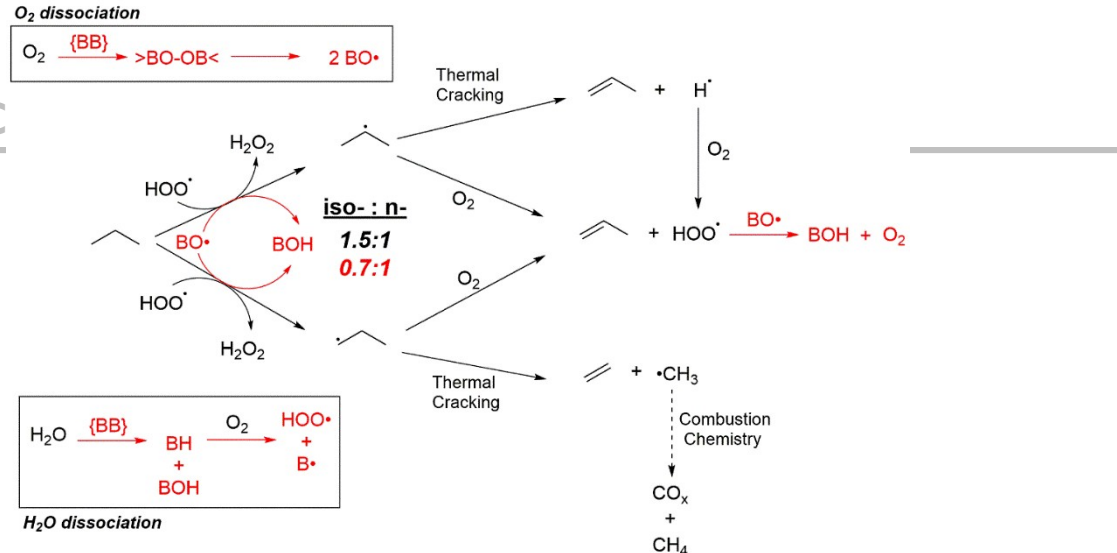
$$\frac{d[C_3H_8]}{dt} = (k_{14}+k_{15})[HOO\bullet][C_3H_8] + (k_{16}$$ (Eq. 2)

Figure 9. Simplified reaction network describing the key reactions involved in the combined surface (red-colored) and gas phase (black-colored) oxidative dehydrogenation of propane to propylene and ethylene. iso- : n- ratios shown in the figure detail the propyl radical distribution of gas phase and surface propane H abstraction. Overoxidation of methyl radicals is expected to follow conventional combustion chemistry routes to form methane and carbon oxides, while at high conversions overoxidation of propylene may lead to additional CO_x formation. H_2O_2 can decompose to form water in the gas phase or $HOO\bullet$ on the catalyst surface as discussed in the text.

We point out that both $HOO\bullet$ and $>BO\bullet$ can either propagate upon reaction with propane or terminate (reactions 6 and 7). This leads to a higher radical quasi steady-state concentration – at a given conversion – at higher propane concentrations, leading to the apparent second order observed for propane (Fig. 1).

From a catalytic materials perspective, we can hypothesize that surface species that can initiate oxidation while also favoring *i*-propyl radical formation would lead to enhanced ODH performance. Indeed, the formation of *n*-propyl radicals inevitably leads to non-negligible formation of C-C cracking products. On the other hand, the more favorable iC_3H_7/nC_3H_7 distribution stemming from gas-phase propane H-abstraction suggests that optimizing the void space in a catalyst bed, as well as the development of catalysts that can generate $HOO\bullet$ radicals rather than alkyl radicals may provide additional benefits during ODH.

Conclusion

The combined surface and gas-phase reaction network provides a sound mechanistic framework for future studies of B-containing materials. While upon first inspection the addition of a gas-phase may prove complex, we have shown that it is the gas-phase component itself that enables the outstanding product distribution observed with boron-based catalysts. This situation, where the surface initiates a free radical gas-phase reaction, stands in sharp contrast with the mechanisms that have been proposed in the literature for vanadium-based catalysts. Indeed, those systems operate *via* a Mars van Krevelen mechanism where oxidized vanadium species presumably homolytically activate a C-H bond of propane.[32] Although never observed experimentally, the nascent radicals are assumed to remain adsorbed to the surface and react consecutively to propylene *via* a second H-abstraction (so-called rebound mechanism), leaving behind a

reduced vanadium surface site. Re-oxidation of the surface with oxygen to regenerate the H-abstracting species is fast and not rate-determining, explaining the zero-order kinetics in oxygen.[17]

Contrasting this reaction mechanism with the one proposed for boron-catalysts in this work highlights two major differences. For the boron-initiated mechanism, a key role of the catalyst is to generate the reactive species ($HOO\bullet$ radicals) that activate the propane substrate in the gas-phase, leading to fast radical propagation. A fraction of the propane reacts directly with the catalyst surface during chain initiation, playing a critical role in establishing the distribution of available propyl species in the gas-phase. This reaction channel in turn lights off a gas-phase reaction and leads to the oxyfunctionalization of the BN surface under ODH conditions. We emphasize that heating BN in the presence of only oxygen does not result in surface oxidation, implying that the oxyfunctionalization goes hand-in-hand with the gas-phase radical chemistry. Our computational studies also highlight the complexity of this oxidation, leading to a variety of boron species with different reactivities. In contrast, the well-studied vanadium-based catalysts are assumed to primarily activate the C-H bond of propane at the surface. This, in combination with stronger interactions of the reaction intermediates with the catalyst surface, and potentially the propylene product, explains the rapid loss in selectivity as the propane conversion increases for vanadium-based catalysts.

We conclude that optimal ODH catalysts should (1) generate reactive H-abstracting species that favor the abstraction of secondary C-H bonds in propane, and (2) not interact strongly with intermediates and products to minimize fast consecutive surface oxidation steps. These conclusions are in line with studies by Iglesia *et al.* exploring $\bullet OH$-mediated oxidation of methane[33] and Deshlahra *et al.* investigating NO_x-mediated ODH reactions[34] and reveal a general set of guidelines to proceed with the development of more selective catalysts.
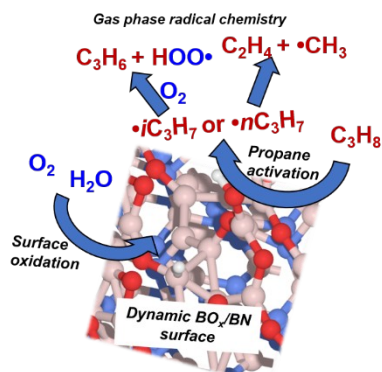
11

Acknowledgements

[1] J. M. Venegas, W. P. McDermott, I. Hermans, *Acc. Chem. Res.* **2018**, *51*, 2556–2564.

[2] J. Tian, J. Lin, M. Xu, S. Wan, J. Lin, Y. Wang, *Chem. Eng. Sci.* **2018**, *186*, 142–151.

[3] L. Shi, Y. Wang, B. Yan, W. Song, D. Shao, A.-H. Lu, *Chem. Commun.* **2018**, *54*, DOI 10.1039/C8CC04604B.

[4] R. Huang, B. Zhang, J. Wang, K.-H. Wu, W. Shi, Y. Zhang, Y. Liu, A. Zheng, R. Schlögl, D. S. Su, *ChemCatChem* **2017**, *9*, 3293–3297.

[5] J. T. Grant, C. A. Carrero, F. Goeltl, J. Venegas, P. Mueller, S. P. Burt, S. E. Specht, W. P. McDermott, A. Chieregato, I. Hermans, *Science (80).* **2016**, *354*, 1570–1573.

[6] P. Chaturbedy, M. Ahamed, M. Eswaramoorthy, *ACS Omega* **2018**, *3*, 369–374.

[7] A. M. Love, B. Thomas, S. E. Specht, M. P. Hanrahan, J. M. Venegas, S. P. Burt, J. T. Grant, M. C. Cendejas, W. P. McDermott, A. J. Rossini, et al., *J. Am. Chem. Soc.* **2019**, *141*, 182–190.

[8] A. M. Love, M. C. Cendejas, B. Thomas, W. P. McDermott, P. Uchupalanun, C. Kruszynski, S. P. Burt, T. Agbi, A. J. Rossini, I. Hermans, *J. Phys. Chem. C* **2019**, *123*, 27000–27011.

[9] Z. Zhang, E. Jimenez-Izal, I. Hermans, A. N. Alexandrova, *J. Phys. Chem. Lett.* **2019**, *10*, 20–25.

[10] J. M. Venegas, J. T. Grant, W. P. McDermott, S. P. Burt, J. Micka, C. A. Carrero, I. Hermans, *ChemCatChem* **2017**, *9*, 2118–2127.

[11] W. P. McDermott, J. Venegas, I. Hermans, *ChemSusChem* **2020**, *13*, 152–158.

[12] J. M. Venegas, I. Hermans, *Org. Process Res. Dev.* **2018**, *22*, 1644–1652.

[13] E. Spier, U. Neuenschwander, I. Hermans, *Angew. Chemie Int. Ed.* **2013**, *52*, 1581–1585.

[14] X. Zhang, R. You, Z. Wei, X. Jiang, J. Yang, Y. Pan, P. Wu, Q. Jia, Z. Bao, L. Bai, et al., *Angew. Chemie Int. Ed.* **2020**, *n/a*, DOI 10.1002/anie.202002440.

[15] K. Takanabe, E. Iglesia, *J. Phys. Chem. C* **2009**, *113*, 10131–10145.

[16] K. Takanabe, S. Shahid, *AIChE J.* **2017**, *63*, 105–110.

[17] K. Chen, A. Khodakov, J. Yang, A. T. Bell, E. Iglesia, *J. Catal.* **1999**, *186*, 325–333.

[18] S. T. Oyama, A. M. Middlebrook, G. A. Somorjai, *J. Phys. Chem.* **1990**, *94*, 5029–5033.

[19] L. Leveles, K. Seshan, J. A. Lercher, L. Lefferts, *J. Catal.* **2003**, *218*, 296–306.

[20] N. R. Altvater, R. W. Dorn, M. C. Cendejas, W. P. McDermott, B. Thomas, A. J. Rossini, I. Hermans, *Angew. Chemie Int. Ed.* **2020**, DOI 10.1002/anie.201914696.

[21] Z. Zhang, B. Zandkarimi, A. N. Alexandrova, *Acc. Chem. Res.* **2020**, DOI 10.1021/acs.accounts.9b00531.

[22] H. Zhai, A. N. Alexandrova, *ACS Catal.* **2017**, *7*, 1905–1911.

[23] L. M. Aparicio, S. A. Rossini, D. G. Sanfilippo, J. E. Rekoske, A. A. Trevino, J. A. Dumesic, *Ind. Eng. Chem. Res.* **1991**, *30*, 2114–2123.

[24] J. T. Grant, W. P. McDermott, J. M. Venegas, S. P. Burt, J. Micka, S. P. Phivilay, C. A. Carrero, I. Hermans, *ChemCatChem* **2017**, *9*, 3623–3626.

[25] J. Tian, J. Tan, M. Xu, Z. Zhang, S. Wan, S. Wang, J. Lin, Y. Wang, *Sci. Adv.* **2019**, *5*, eaav8063.

[26] L. Shi, B. Yan, D. Shao, F. Jiang, D. Wang, A.-H. Lu, *Chinese J. Catal.* **2017**, *38*, 389–395.

[27] C. A. Carrero, R. Schloegl, I. E. Wachs, R. Schomaecker, *ACS Catal.* **2014**, *4*, 3357–3380.

[28] H. J. Curran, *Int. J. Chem. Kinet.* **2006**, *38*, 250–275.

[29] R. S. Konar, R. M. Marshall, J. H. Purnell, *Trans. Faraday Soc.* **1968**, *64*, 405.

[30] J. Warnatz, in *Combust. Chem.*, Springer New York, New York, NY, **1984**, pp. 197–360.

[31] W. Tsang, *J. Phys. Chem. Ref. Data* **1988**, *17*, 887–951.

[32] X. Rozanska, R. Fortrie, J. Sauer, *J. Phys. Chem. C* **2007**, *111*, 6041–6050.

[33] K. Takanabe, E. Iglesia, *Angew. Chemie Int. Ed.* **2008**, *47*, 7689–7693.

[34] L. Annamalai, Y. Liu, P. Deshlahra, *ACS Catal.* **2019**, *9*, 10324–10338.

RESEARCH ARTICLE

Entry for the Table of Contents

Gas phase radical chemistry

C_3H_6 + HOO• C_2H_4 + •CH_3

O_2

•iC_3H_7 or •nC_3H_7 C_3H_8

Propane activation

O_2 H_2O

Surface oxidation

Dynamic BO_x/BN surface

The origin of high propylene selectivity during hBN-catalyzed ODH stems from surface-initiated radical reactions that propagate *via* gas phase chemistry. This reaction network contrasts with previously studied vanadium-based catalysts where surface reactions predominate, lowering selectivity. An approach consisting of experimental and computational investigations brings a first look at this complex surface-gas phase reaction network.

Institute and/or researcher Twitter usernames:

University of Wisconsin - Madison - @UWMadison

University of Wisconsin - Madison Department of Chemistry @UWMadisonChem

Hermans Group - @hermansgroup

University of California, Los Angeles - @UCLA

University of California, Los Angeles Department of Chemistry and Biochemistry @UCLAchem